

High Dynamic Range Reduction Via Maximization of Image Information

A. Ardeshir Goshtasby*

Abstract—An algorithm for blending multiple-exposure images of a scene into an image with maximum information content is introduced. The algorithm partitions the image domain into subimages and for each subimage selects the image that contains the most information about the subimage. The selected images are then blended together using monotonically decreasing blending functions that are centered at the subimages and have a sum of 1 everywhere in the image domain. The optimal subimage size and width of blending functions are determined in a gradient-ascent algorithm that maximizes image information. The proposed algorithm reduces dynamic range while preserving local color and contrast.

Index Terms—High-dynamic range image, image blending, image information, color image, multiple-exposure image

1 Introduction

With recent advances in photography [5] and sensor technology [21] [33], high dynamic range images are becoming more commonly available. In order to view such images on low dynamic range displays, methods to reduce the dynamic range of images have been developed. Dynamic range reduction methods typically start from a floating-point image and arrive at a byte image that is suitable for display on regular monitors. In this work, rather than starting from a floating-point image, a set of byte images obtained at multiple

*Department of Computer Science and Engineering, Wright State University, Dayton, OH 45435. E-mail: ardeshir@cs.wright.edu

exposures of a scene are used. Red, green, and blue values in an image are assumed to vary between 0 and 255. This enables combining images captured by regular cameras into highly informative images for display on regular monitors.

When lighting across a scene varies greatly, there are image areas that appear over-exposed or under-exposed no matter what shutter speed is used. Given a set of images obtained at multiple exposures of a scene, the image domain is subdivided into small subimages, and the input image providing the most information within each subimage is selected. A subimage, therefore, has an associating image, which contains more information about the subimage than any other image in the input. The images selected in this manner are multiplied by blending functions and added together to produce the output. A blending function, which is a monotonically decreasing function, is centered at a subimage within the associating image. The blending functions are defined such that their sum is 1 everywhere in the image domain. The blending functions select well-exposed and highly informative areas in input images while excluding under-exposed and over-exposed image areas that hardly carry any information. The method aims to produce an image that is highly informative everywhere.

In the following, after reviewing related work, details of the proposed method are given. Then, experimental results are presented and compared with those obtained by two recent high dynamic range reduction methods.

2 Related Work

The problem of high dynamic range reduction has been studied considerably in image processing. Noting that lighting variations occur at low spatial frequencies and the human visual system is more sensitive to mid and high frequencies, Oppenheim et al. [23] and Stockham [27] developed methods that would attenuate the low spatial frequencies while enhancing the mid and high frequencies. The method performs a histogram modification followed by a logarithmic mapping that reassigns the image intensities to enhance details in darker areas

at the cost of obtaining lower contrast in brighter areas.

A linear mapping developed by Ward [31] preserves visible changes in luminances between input and output at a particular fixation point. The mapping clips very high and very low values that belong to a very small number of image pixels in order to maintain apparent contrast and visibility. To determine similar maps, Tumblin and Rushmeier [29] used models of the human visual system. They developed an operator based on a brightness function that could reduce dynamic range while preserving the overall impression of brightness. Larson et al. [19], rather than mapping image luminances based on spatial locations, identified clusters of adaptation levels and developed a mapping function that would preserve local contrast and visibility. Models of contrast sensitivity, glare, and color sensitivity of the human visual system were used to further improve visibility and appearance of the output.

These methods provide a one-to-one mapping between luminance values in input and luminance values in output. They are very efficient and work well when dynamic range in input is not very high. When dynamic range in input is very high, global methods lose apparent contrast and methods that use different mapping functions for different image regions are required. In a method developed by Chiu et al. [4], luminance values were scaled based on spatial averaging of luminances in local neighborhoods. Then, values in bright and dark areas were scaled differently based on their spatial locations. Since the human visual system is less sensitive to low spatial frequencies than to mid and high frequencies, a variable scaling was employed to slowly vary local contrast while reducing global dynamic range. This method, however, may produce gradient reversals that produce haloing effects around bright areas. A spatially varying tone-mapping method has been developed by Schlick [26] that also behaves like Chiu et al.'s method but is computationally more efficient.

Another spatially varying tone-mapping approach that behaves like Chiu et al.'s method is the method of Jobson et al. [17], which extends the Land's Retinex model [18] to achieve simultaneous dynamic range reduction, color constancy, and brightness rendition. To avoid visible gradient reversals that cause halos, they further took into consideration the image

content. Ferwerda et al. [10] developed a computational model of visual adaptation that was based on psychophysical experiments. The model takes into consideration changes in threshold visibility, color appearance, visual acuity, and temporal sensitivity of the human visual system. Pattanaik et al. [24] decomposed the high dynamic range into multiscale and used pyramids built with bilinear filters to faithfully reproduce properties of the human visual system. The model accounted for changes in threshold visibility, visual acuity, color discrimination, colorfulness, and apparent contrast. This method, however, still produces haloing effects around bright spots.

A high dynamic range reduction method that does not produce haloing effects is developed by Tumblin and Turk [30]. The method creates a hierarchy of progressively more detailed regions and boundaries. Then the contrast between large regions is reduced and details in small regions are added to them. Since boundaries at different levels are not smoothed, halos are not obtained. Fattal et al. [9] work in the gradient space. Noting that a high change in lighting across a scene results in high gradients and that fine details due to change in scene reflectances result in smaller gradients, they reduced high gradients to reduce dynamic range in luminances. In the same spirit, Durand and Dorsey [8] use bilateral filters to separate details and large features into a detailed layer and a base layer. The base layer encodes large luminance variations while the detailed layer represents variations due to local luminance changes. By reducing contrast in the base layer, large luminance variations across the image are reduced. An image with reduced dynamic range is then created from the revised base layer and the detailed layer. Ashikhmin [2] achieves the same by first finding local adaptation luminance at each point and reducing the display range through a mapping process. Since this mapping could lose important image details, the details are then added to the obtained image to reproduce local image details while keeping the dynamic range low. A method developed by Tumblin et al. [28] first builds a display image from several layers of lighting and surface properties. Then, only the lighting layers are compressed to reduce contrast while maintaining image details. This method is suitable for synthetic images where

the layers can be created from scene and lighting information.

The above provided a brief review of high dynamic range reduction methods. For a more thorough review of the methods see the excellent survey papers by DiCarlo and Wandell [7] and Devlin et al. [6]. It should also be mentioned that photographic techniques for high dynamic range reduction have been around even before the digital media [32]. Reinhard et al. [25] recently reported a method for automating the manual Zone System photographic method [1], which achieves what photographers and artists have been achieving by manual means throughout the years.

In this paper, a high dynamic range reduction method is introduced that is based on the observation that if lighting across a scene varies greatly, when images at multiple exposures are obtained an image area may appear the most informative in one image than in any other image. Under-exposed and over-exposed areas in an image carry very little information while areas in an image that have received the right amount of exposure carry the most information. A method is introduced that blends the images together in such a way that over-exposed and under-exposed areas in the images are excluded while keeping areas that are well exposed and are highly informative.

3 Approach

The problem to be solved is as follows: Given N images of a static scene obtained by a stationary camera at different exposure levels, it is required to blend the images together in such a way that the obtained image has the maximum information content. Image information will be measured using image entropy [3] [11]. The higher the entropy of an image, the more informative the image will be. In image processing, maximization of image entropy has been used as a means to enhance images [3] [14]. To maximize entropy, intensities in the input have been mapped to intensities in the output in such a way to produce a flat histogram. A flat histogram results in intensities that are equally likely to appear in an image.

The approach taken here is different from earlier approaches in that, rather than remap-

ping image luminances to a lower range, the most informative subimages in each image are selected and then smoothly combined to produce the output. When brightness across a scene varies greatly so that images at various exposures are needed to capture all scene details, the main problem becomes that of identifying the image that contains the most detail or information about a particular scene area. An image that is over-exposed or under-exposed within an area of interest does not contain as much information as an image that is perfectly exposed.

In a gray scale image, entropy is computed from

$$E_g = \sum_{i=0}^{255} -p_i \log(p_i), \quad (1)$$

where p_i is the probability that if a pixel is randomly selected in the image it will have intensity i . To estimate $\{p_i : i = 0, \dots, 255\}$, first the histogram of the image is computed. Assuming the number of pixels having intensity i is n_i and the image contains n pixels, $p_i = n_i/n$.

The human visual system is capable of discriminating far more colors than luminances [15]. Therefore, it makes sense to compute image information using all color components rather than only the luminance component. The entropy of a color image is computed from

$$E_c = \sum_{i=0}^{255} -p_i^r \log(p_i^r) + \sum_{i=0}^{255} -p_i^g \log(p_i^g) + \sum_{i=0}^{255} -p_i^b \log(p_i^b), \quad (2)$$

where r , g , and b denote the red, green, and blue color components, and p_i^r represents the probability that when a random pixel is selected in the red component of the image, the intensity of the pixel will be i . Similarly, p_i^g and p_i^b are defined using the green and blue components of the image.

To determine the image that has the best exposure for a given local neighborhood among all N input images, first the images are subdivided into blocks of size $d \times d$. d will be one of the unknown parameters of the method to be determined by maximizing information content in the output. Image entropy E_c is determined for each block in each of the N images, and

the image that produces the highest entropy for a block is selected to represent that block in the output.

If we simply create an image from the composition of image blocks obtained in this manner, we will obtain an image that may contain sharp discontinuities across image blocks. Although each block will be very informative, the image composed from them will be awkward to view. An example is shown in Fig. 1. Figures 1a–e show a set of images of an office room taken at five different exposure levels. These images are of size 480×640 pixels. Dividing the images into blocks of 160×160 pixels, we obtain an array of 3×4 or 12 blocks. If we calculate the entropy within each block for the five input images, cut out the block containing the highest entropy among all images, and put the blocks back together, we obtain the image shown in Fig. 1f.

To remove discontinuities across image blocks, instead of composing the blocks into an image, the images representing the blocks are blended together. A monotonically decreasing blending function is centered at each block and image colors are multiplied by corresponding blending function values. Therefore, the color at a pixel in the output is obtained from a weighted sum of colors at the same pixel in different images in the input. A blending function assigns the maximum weight to the pixel at the center of a selected block in an image, and it assigns smaller weights to other pixels proportional to the inverse distances of the pixels to the block center.

Assuming N images are given, each image has been subdivided into an array of $n_r \times n_c$ blocks, j and k denote the row and column indices of the blocks, and \mathbf{I}_{jk} denotes the image that has the highest entropy among N images for block jk , we compute output image $\mathbf{O}(x, y)$ from

$$\mathbf{O}(x, y) = \sum_{j=1}^{n_r} \sum_{k=1}^{n_c} W_{jk}(x, y) \mathbf{I}_{jk}(x, y), \quad (3)$$

where $W_{jk}(x, y)$ is the value of the blending function centered at the jk th block at (x, y) , and $\mathbf{I}_{jk}(x, y)$ is a vector representing the color coordinates of image \mathbf{I}_{jk} at (x, y) . Note that the number of images being blended is equal to the number of blocks and not the number

of input images. When the blocks are small, many blocks may be selected from the same image. Also note that, rather than using image values within only selected blocks, entire images are blended together, although contribution of far away blocks on a pixel may be very small. This process smoothly blends the images, avoiding creation of discontinuities across image blocks.

Since the blocks form a uniform grid, tensor-product blending functions, such as B-splines [12], may be used. When B-spline blending functions are centered at the blocks, the blending functions will smoothly blend the images. This works for interior blocks, but for blocks that touch the image borders, the sum of the weights will be less than 1, making the border blocks darker than what they should be. We will need blending functions that extend over the entire image domain and have a sum of 1 everywhere. Blending functions that provide this property are the rational Gaussian (RaG) blending functions [13]. RaG blending functions are defined by

$$W_{jk}(x, y) = \frac{G_{jk}(x, y)}{\sum_{j=1}^{n_r} \sum_{k=1}^{n_c} G_{jk}(x, y)}, \quad (4)$$

where $G_{jk}(x, y)$ represents the value of a Gaussian of height 1 centered at the jk th block at (x, y) :

$$G_{jk}(x, y) = \exp \left\{ -\frac{(x - x_{jk})^2 + (y - y_{jk})^2}{2\sigma^2} \right\}. \quad (5)$$

(x_{jk}, y_{jk}) are the coordinates of the center of the jk th block, and σ is the standard deviation or the width of the Gaussians. In the following, we will refer to σ as the width of the blending functions.

Figure 1g shows the image obtained by centering blending functions of width 80 pixels at blocks of size 160×160 pixels in the selected images and multiplying color values at image pixels with weights given by the blending functions and adding the weighted colors together. This will be the kind of output we will generate. σ is one other unknown parameter that has to be determined to maximize information content in the output. Since more than one image block may point to the same image, an image may be used more than once in relation

(3). The blending functions blend the proper amounts of the input images to create the output.

There are two parameters to be determined in the proposed method: d , image block size, and σ , width of the blending functions. As these parameters are varied, different images will be obtained. We have to determine the d and σ that maximize image entropy as computed by relation (2). Experiments on various images have shown that the plot of entropy as a function of d and σ has a single peak. Therefore, a gradient-ascent algorithm can find the optimal parameters. We first fix parameter σ and find the optimal d . Then, knowing the optimal d , we find the optimal σ .

The following summarizes the steps of the proposed algorithm.

Algorithm BLEND:

1. Set block size d and width of blending functions σ to some initial guesses, and let Δ be the increment in d and σ .
2. Determine the entropy of block jk in each image using formula (2) for $j = 1, \dots, n_r$ and $k = 1, \dots, n_c$ and let the image having the highest entropy within block jk be \mathbf{I}_{jk} .
3. Find the entropy of the image obtained by blending the images selected by the blocks in Step 2 with blending functions of width σ .
4. By incrementing or decrementing d by Δ in the gradient-ascent direction and repeating Steps 2 and 3, find that d which produces the highest entropy. Let the obtained d be d_{max} .
5. Letting $d = d_{max}$ and incrementing or decrementing σ by Δ in the gradient-ascent direction, determine that σ which produces the maximum entropy in Step 3. Let the obtained σ be σ_{max} .
6. Select the images identified by Step 2 when setting $d = d_{max}$, and create a new image by blending the selected images with blending functions of width σ_{max} .

The initial values for parameters d and σ are set to the averages of optimal parameters found in a number of test runs of the algorithm. Applying this algorithm to images 1a–e, we obtain the image shown in Fig. 1h. As initial values, $d = 128$ pixels and $\sigma = 96$ pixels were used, and Δ was 32 pixels. d_{max} and σ_{max} obtained by the algorithm were 224 and 128 pixels, respectively. Smaller increments produce higher optimal entropies at a higher computational cost. For images 1a–e, increments smaller than 32 do not increase the optimal entropy by a significant amount, but they slow down the computations considerably. Also, increments larger than 32 pixels, although speeding up the process considerably, lower the image entropy enough to be noticeable. This parameter should be chosen as a compromise between speed and accuracy. For the images used in this paper, Δ was 32 pixels and initial values for d and σ were 128 and 96 pixels, respectively.

4 Results and Discussion

To determine the quality of images obtained by the proposed method and to compare the results with those obtained by existing methods, a number of experiments were carried out. Figure 2 shows images of a waiting room. The top row shows the original images representing different exposures of the room. The bottom-left image shows the result obtained by Fattal et al. [9], and the bottom-right image shows the result obtained by the proposed method. The image produced by Fattal et al. shows more details underneath the lights, while the image produced by the proposed method shows more details underneath the chairs and the image has an overall high contrast. Comparing the results to the original images, we see that the proposed method has more faithfully reproduced color and contrast, while the method of Fattal et al. has changed the colors.

Figure 3 shows a comparison of the proposed method with manual photographic tone reproduction techniques. The two images on the top show the original images, the middle image shows the result obtained by manual photographic techniques [20], and the image on the bottom shows the result obtained by the proposed method. The photographic and

proposed methods have both preserved color and contrast of the original images and the results are virtually indistinguishable, except for a slightly brighter foreground in the manually created image.

The images in the left column in Fig. 4 represent nine images of Belgium House obtained at different exposure levels. The three images in the right column from top to bottom show results obtained by the methods of Tumblin and Turk [30] and Fattal et al. [9], and our method. Each method has its own characteristics. Tumblin and Turk’s method has recovered very small scene details, some even not visible in the original images. The method of Fattal et al. has created very vivid colors in bright areas in the scene, some even nonexistent in the original images. The proposed method has reproduced color and contrast as they appear in the input.

The top row in Fig. 5 shows fifteen images of the Memorial Church obtained at different exposure levels. The three images below that show results obtained by Tumblin and Turk, Fattal et al., and us. Comparison of the results is very subjective. Depending on what a viewer wants to see in the obtained image, the viewer may choose one result over the other two. Tumblin and Turk’s method has reproduced very small details in the scene but the overall contrast is not very high. The method of Fattal et al. has picked up main details in the scene and has a higher contrast. The method proposed here has reproduced scene highlights, causing some colors to appear less saturated than those obtained by the other two methods. An observer entering the scene will initially see the highlights. Gradually, when the eyes adapt to the high intensities, the observer can distinguish different colors within the highlights. The proposed method has generated an overall higher contrast image than the other two methods. Also, the proposed method has produced colors in the output that are more similar to those in the input. The methods of Tumblin and Turk and Fattal et al. by changing only the luminances change perceived colors. This happens because the contrast sensitivity of the achromatic channel in the human visual system as a function of the spatial frequency is like a bandpass filter, and the contrast sensitivity of the red/green

or the yellow/blue channel is like a lowpass filter [22], causing local mapping methods that work on image luminances change color appearance in the output.

The last example is depicted in Fig. 6. There are eleven original images shown in the top row. Results obtained by Tumblin and Turk, Fattal et al., and the proposed method are shown, respectively, from left to right in the bottom row. Tumblin and Turk’s method has picked up some of the very small scene details at the cost of missing some of the larger details, such as the fallen leaves in the foreground. The method of Fattal et al. has done a very good job of recovering scene details, even the fallen leaves in the foreground. The proposed method has produced an overall higher contrast image than the other two methods. It has picked up more details in bright scene areas than Fattal et al.’s method, and by comparing the output with the original images we observe that the proposed method has reproduced scene colors more accurately than the method of Fattal et al.

The computational complexity of the algorithm depends on 1) image size, 2) initial block size and standard deviation of Gaussians, and 3) increment in block size and standard deviation in Algorithm BLEND. For the images used in this paper, computation time varied between 15 seconds and 4 minutes. The small images shown in Fig. 2 (231×343 pixels) required approximately 15 seconds for processing and the large images shown in Fig. 3 (1024×1536 pixels) required about 4 minutes. These times are measured on an SGI O2 computer with an R10000 processor and 256 MB internal memory.

5 Summary and Conclusions

A new method for reducing high dynamic range in color images was presented. The method subdivides the image domain into small blocks and for each block selects the image that provides the most information within that block. The images selected for each block are then blended together to produce the output. The block size and the width of the blending function are determined in a gradient-ascent algorithm to maximize information content in the output.

Image information is computed using all three color components rather than only the luminance. As a result, the images produced by the proposed method contain considerable color details. This method preserves scene highlights if color information in a highlight area is quite high.

Results by the proposed method were compared with a manual photographic method as well as two well-known automatic methods. The proposed method produces results that are comparable to those obtained by the manual photographic method. Experimental results also show that the proposed method preserves local color and contrast better than the two automatic methods.

Acknowledgements

The author would like to thank Shree Nayar, Max Lyons, Dani Lischinski, Paul Debevec, and Jack Tumblin for providing the original images used in the experiments in Figs. 2–6. The author also would like to thank Toni Larson for helping with the implementation of Algorithm BLEND. This work was supported in part by the Ohio Board of Regents.

References

- [1] A. Adams, *The Print*, The Ansel Adams Photography Series, The Little, Brown, and Company, 1983.
- [2] M. Ashkhmin, “A Tone Mapping Algorithm for High Contrast Images,” *Eurographics Workshop on Rendering*, P. Debevec and S. Gibson (eds.), 1–11, 2002.
- [3] K. R. Castleman, *Digital Image Processing*, Prentice Hall, 569–570, 1996.
- [4] K. Chiu, M. Herf, P. Shirley, S. Swamy, C. Wang, and K. Zimmerman, “Spatially Nonuniform Scaling Functions for High Contrast Images,” *Proceedings of Graphics Interface*, 245–253, 1993.

- [5] P. E. Debevec and J. Malik, "Recovering High Dynamic Range Radiance Maps from Photographs," *Proceedings of SIGGRAPH 1997*, ACM Press / ACM SIGGRAPH, 369–378, 1997.
- [6] K. Devlin, A. Chalmers, A. Wilkie, and W. Purgathofer, "Tone Reproduction and Physically Based Spectral Rendering," *Eurographics, STAR*, 101–123, 2002.
- [7] J. M. DiCarlo and B. A. Wandell, "Rendering High Dynamic Range Images," *Proceedings of the SPIE: Image Sensors*, vol. 3965, 392–401, 2000.
- [8] F. Durand and J. Dorsey, "Fast Bilateral Filtering for the Display of High-Dynamic-Range Images," *Proceedings of ACM SIGGRAPH*, 257–266, 2002.
- [9] R. Fattal, D. Lischinski, and M. Werman, "Gradient Domain High Dynamic Range Compression," *Proceedings of ACM SIGGRAPH*, 249–256, 2002.
- [10] J. A. Ferwerda, S. N. Pattanaik, P. Shirley, and D. P. Greenberg, "A Model of Visual Adaptation for Realistic Image Synthesis," *Proceedings of SIGGRAPH 1996*, ACM Press / ACM SIGGRAPH, 249–258, 1996.
- [11] B. R. Frieden, "Restoring with Maximum Likelihood and Maximum Entropy," *J. Optical Society America*, vol. 62, 511–518, 1972.
- [12] W. J. Gordon and R. Riesenfeld, "B-spline Curves and Surfaces," *Computer Aided Geometric Design*, R. Barnhill and R. Riesenfeld, 95–126, 1974.
- [13] A. Goshtasby, "Design and Recovery of 2-D and 3-D Shapes Using Rational Gaussian Curves and Surfaces," *Int'l J. Computer Vision*, vol. 10, no. 3, 233–256, 1993.
- [14] E. L. Hall, "Almost Uniform Distributions for Computer Image Enhancement," *IEEE Trans. Computers*, vol. 23, no. 2, 207–208, 1974.
- [15] E. L. Hall, *Computer Image Processing and Recognition*, Academic Press, 29–30, 1979.

- [16] B. Hill, Th. Roger, and F. W. Vorhagen, “Comparative Analysis of the Quantization of Color Spaces on the Basis of the CIELAB Color-Difference Formula,” *ACM Trans. Graphics*, vol. 11, no. 4, 373–405, 1992.
- [17] D. J. Jobson, Z. Rahman, and G. A. Woodell, “A Multiscale Retinex for Bridging the Gap Between Color Images and the Human Observation of Scenes,” *IEEE Trans. Image Processing*, vol. 6, no. 7, 965–976, 1997.
- [18] E. H. Land, “The Retinex Theory of Color Vision,” *Scientific American*, vol. 237, no. 6, 1997.
- [19] G. W. Larson, H. Rushmeier, and C. Piatko, “A Visibility Matching Tone Reproduction Operator for High Dynamic Range Scenes,” *IEEE Trans. Visualization and Computer Graphics*, vol. 3, no. 4, 291–306, 1997.
- [20] Max Lyons, Personal Communication, 2002.
- [21] T. Mitsunaga and S. K. Nayar, “High Dynamic Range Imaging: Spatially Varying Pixel Exposures,” *Proceedings of the Computer Vision and Pattern Recognition*, 472–479, 2000.
- [22] K. T. Mullen, “The Contrast Sensitivity of Human Color Vision to Red-Green and Blue-Yellow Chromatic Gratings,” *J. Physiol.*, vol. 359, 381–400, 1985.
- [23] A. V. Oppenheim and R. Schafer, “Nonlinear Filtering of Multiplied and Convolved Signals,” *Proceedings of the IEEE*, vol. 56, no. 8, 1264–1291, 1968.
- [24] S. N. Pattanaik, J. A. Ferwerda, M. D. Fairchild, and D. P. Greenberg, “A Multiscale Model of Adaptation and Spatial Vision for Realistic Image Display,” *Proceedings of SIGGRAPH 1998*, ACM Press / ACM SIGGRAPH, 287–298, 1998.

- [25] E. Reinhard, M. Stark, P. Shirley, and J. Ferwerda, “Photographic Tone Reproduction for Digital Images,” *Proceedings of ACM SIGGRAPH 2002*, ACM Trans. Graphics, vol. 21, no. 3, 267–276, 2002.
- [26] C. Schlick, “Quantization Techniques for Visualization of High Dynamic Range pictures,” *Proceedings of the Fifth Eurographics Workshop on Rendering*, 7–20, 1994.
- [27] T. G. Stockham, “Image Processing in the Context of a Visual Model,” *Proc. IEEE*, vol. 60, no. 7, 828–842, 1972.
- [28] J. Tumblin, J. K. Hodgins, and B. K. Guenter, “Two Methods for Display of High Contrast Images,” *ACM Trans. Graphics*, vol. 18, no. 1, 59–94, 1999.
- [29] J. Tumblin and H. E. Rushmeier, “Tone Reproduction for Realistic Images,” *IEEE Computer Graphics and Applications*, vol. 13, no. 6, 42–48, 1993.
- [30] J. Tumblin and G. Turk, “LCIS: A Boundary Hierarchy for Detail-Preserving Contrast Reduction,” *Proceedings of SIGGRAPH*, ACM Press / ACM SIGGRAPH, 83–90, 1999.
- [31] G. J. Ward, “A Contrast-Based Scale Factor for Luminance Display,” P. E. Heckbert (ed.), *Graphics Gems IV*, Academic Press Professional, 415–421, 1994.
- [32] J. C. Woods, *The Zone System Craftbook*, McGraw Hill, 1993.
- [33] D. Yang, A. E. Gamal, B. Fowler, and H. Tian, “A 640×512 CMOS Image Sensor with Ultra Wide Dynamic Range Floating-Point Pixel-Level ADC,” *IEEE J. Solid State Circuits*, vol. 34, no. 12, 1821–1834, 2000.



Figure 1: (a)–(e) Images representing different exposures of an office room. (f) The image obtained by composing the twelve subimages (image blocks) cut out of the five images. (g) The image produced by centering the blending functions at the selected blocks in the images, multiplying the blending functions with image colors, and adding the weighted colors together. (h) The most informative image constructed from images (a)–(e).



Figure 2: The top row shows five images obtained at different exposures of a waiting room, the bottom-left shows the result obtained by the method of Fattal et al. [9], and the bottom-right shows the result obtained by the proposed method. Original images are courtesy of Shree Nayar.



Figure 3: On the top, two original images of Scottish Highlands obtained at different exposures are shown. The image in the middle shows the result obtained by Max Lyons [20] by manual photographic techniques. The image in the bottom shows the result obtained automatically by the proposed method. The original images are courtesy of Max Lyons.



Figure 4: The left column shows nine images representing different exposures of Belgium House, and the three images in the right column from top to bottom show results obtained by the methods of Tumblin and Turk [1999] and Fattal et al. [2002], and our method. Original images are courtesy of Dani Lischinski.

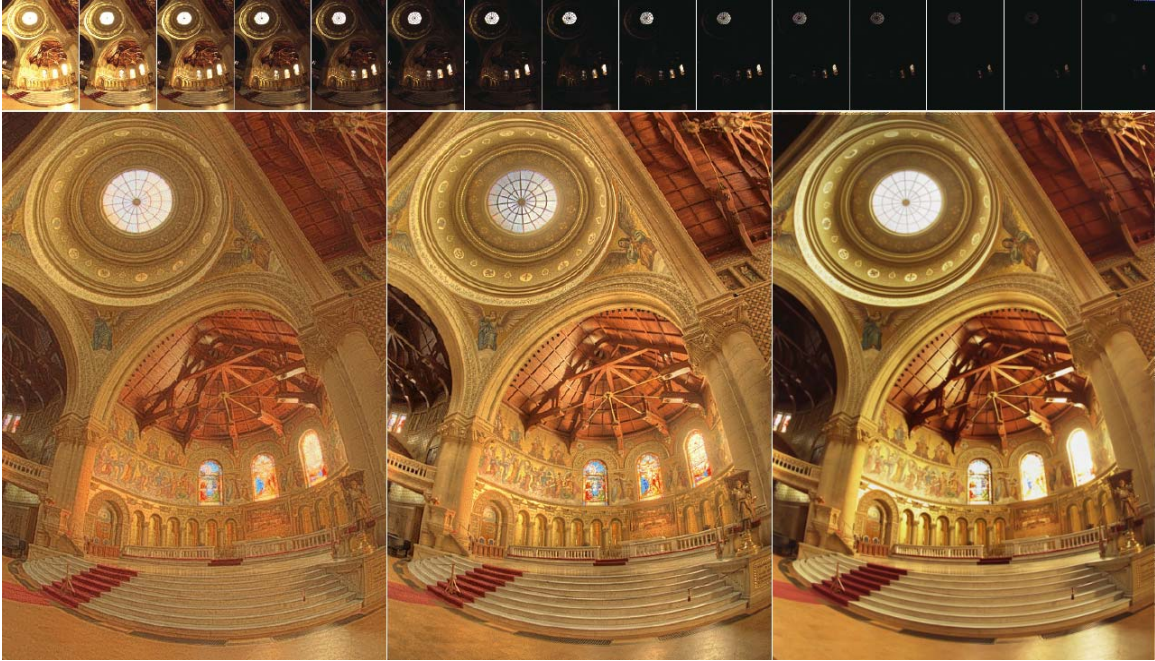


Figure 5: The top row shows fifteen original images, and the images below that from left to right show results obtained by Tumblin and Turk, Fattal et al., and us. Original images are courtesy of Paul Debevec.



Figure 6: The top row shows eleven original images, and the images below that from left to right show the results obtained by the methods of Tumblin and Turk, and Fattal et al., as well as our method. The original images are courtesy of Jack Tumblin.